

## ACTUATION ENHANCEMENT OF A MICRO BIMORPH THERMAL ACTUATOR

Farid Ullah Khan\*

### ABSTRACT

*A bimorph thermal actuator (BTA) is typically used to actuate other MEMS structures, such as, micro-mirrors, atomic force microscope probe tips, membranes of micro pumps and micro valves, etc. This research is focused on enhancing BTA actuation characteristics. The mathematical model for BTA is used to study the behaviour of a spectrum of material combinations. Although a silicon-aluminum (SiO<sub>2</sub>-Al) BTA exhibits superior characteristics over a limited operational range, it is found that a silicon-stainless steel (Si-SS) bimorph provides larger deflections at higher operational conditions. The practical constraints on traditional bimorph materials in extreme operating conditions arise from intrinsic material properties such as yield strength and melting temperature. Under such extreme conditions Si-SS bimorphs perform well, opening up new field applications for this micro device.*

*In order to fabricate the novel Si-Steel bimorph, a generic fabrication sequence is described according to criteria of reproducibility, batch fabrication, applicability and cost effectiveness with the use of newer micro fabrication techniques such Pulsed Laser Deposition (PLD), Laser Ablation (LA) and Micro electro-discharge machining ( $\mu$ EDM). Different designs of bimorph thermally actuated digital micro-mirror devices (DMDs) are also fabricated by the same generic fabrication process in order to show the practical utility of this research in the field of MEMS. The DMDs actuated by BTAs, are easy to fabricate and can scan through larger angles as compared to electrostatically actuated DMDs.*

**KEYWORDS:** *Actuation enhancement, Bimorph, Micro scale, Harsh environment, Thermal actuator.*

### INTRODUCTION

The usage and applications of micro actuators (MAs) have been rapidly increased in recent years. Several MAs have been developed, such as, piezoelectric MA<sup>1</sup>, electrostatic MA<sup>2</sup>, thermal MA<sup>3</sup> and electromagnetic MA<sup>4</sup>. The advantage of thermal MA over the others is the generation of large deflections and high forces. Most of the developed thermal MAs are bimorphs. The actuation mechanism of bimorph thermal actuators (BTAs) is based on the significant difference in the thermal expansion coefficients of the materials used. This is sometimes referred to as the bimetallic effect, as relatively large bimorphs used in applications, such as, thermostats, thermometers, clocks and heat engines are typically fabricated from steel and copper. The BTA, comprised of dual layer of dissimilar materials, that, when subjected to a change in temperature, utilize the mismatch-stresses and mismatch-strains produced by the difference in expansion rates of the bonded materials to provide an actuation force or displacement. The tip deflection and the radius of curvature of the BTA is the function of the temperature, thickness and the material's Young's modulus<sup>5,6,7</sup>. Actuation can also be controlled

by shape and cross-section of the beam<sup>8,9,10</sup>. Moreover, residual stresses in the beam also have a large affect on the tip deflection and can be utilized to manipulate the actuation<sup>11</sup>. Hence the actuation in the BTA could be manipulated by precisely varying the layers thickness, residual stresses and by the proper selection of layers material.

In normal circumstances BTAs are fabricated using standard integrated circuit (IC) fabrication processes. However convenient, this also limits the choice of materials to be joined together, thereby restricting the range of attainable actuation (force or displacement). By identifying process requirements that would allow the use of materials that expand the range of available actuation by virtue of a larger difference in thermal expansion coefficients, higher yield strengths or higher melting temperatures, the feasibility of the enhancement of forces or displacements at the tip of the actuator may be ascertained.

The main advantages of a thermal actuator over other actuator types are ease of fabrication and the relatively large forces produced by these actuators. These

---

\* *Institute of Mechatronics Engineering, University of Engineering & Technology, Peshawar, 25120, Pakistan*

advantages have led the thermal actuators being widely used to both actuate other MEMS devices and for a wide range of specialized applications, such as, flow control in micro-fluidics. Due to its 'prime mover' for MEMS devices, research into improving BTA performance (i.e. increased tip deflection or actuation force) is on-going. Materials and fabrication techniques differing from the conventional BTA fabrication solution-space present an intriguing avenue to device enhancement.

Such research relies on understanding and modeling the behaviour of bimorphs. Werner Riethmuller et al. derived an empirical formula for the radius of curvature of bimorph, when it is heated electrically<sup>6</sup>. Wen-Hwa Chu et al have done the mathematical modeling and derived a relation between tip deflection and change in temperature by using a simple analytical approach, the model being verified by comparison of the finite element analysis with published experimental data<sup>7</sup>.

It is worthwhile to survey some uses of BTAs and the materials used. David Bullen et al, used BTA for parallel dip-pin nanolithography. In dip-pen nanolithography (DPN), nanoscale chemical patterns are created by directly transferring chemical molecules from the tip of an atomic force microscope probe to a surface. They reported the development of a thermally actuated probe array for DPN applications. Silicon nitride ( $\text{Si}_3\text{N}_4$ ) and gold (Au) are used as the materials for the developed BTA. The array consisted of ten thermal bimorph actuated probes, each 300  $\mu\text{m}$  long, with a lateral spacing of 100  $\mu\text{m}$ . The probes are actuated by passing DC current through a heater embedded in the probe base. The array is demonstrated by simultaneously writing ten different octadecanethiol patterns on a gold surface<sup>12</sup>.

Ankur et al., reported a novel large vertical displacement (LVD) microactuator that can generate large piston motion and bi-directional scanning at low driving voltage<sup>13</sup>. Deep reactive ion etching (DRIE), and post-CMOS micromachining process are used for fabrication of the actuator. The BTA is composed of aluminum and silicon dioxide with an embedded polysilicon thermal heater. With a size of only 0.7 mm x 0.32 mm, the LVD micro-mirror demonstrated a vertical displacement of 0.2 mm at 6V DC. With the use of two BTAs, micro-mirror is used to perform bi-directional, rotational scanning. The micro-mirror rotates over  $\pm 15^\circ$  at less than 6V DC, and

over  $\pm 43^\circ$  (that is, greater than  $170^\circ$  optical scan angle) at its resonant frequency of 2.6 kHz.

To achieve multi-degree actuation of the micro-mirror<sup>14</sup>, Shane T Todd et al used an inverted-series-connected (ISC), Al-SiO<sub>2</sub> BTAs. The micro-mirror can operate in one-dimensional (1D) piston-mode and two-dimensional (2D) tilt-mode. Analytical models for the piston-mode and tilt-mode actuations are compared to FEM simulation results. The device was fabricated using the 1.5 $\mu\text{m}$  CMOS process followed by a post-CMOS micromachining for the device release. The displacement versus temperature of the micro-mirror was measured experimentally and compared to analytical and FEM simulation results. Experimental results showed that the micro-mirror displaced by 56  $\mu\text{m}$  at an applied temperature of 150  $^\circ\text{C}$ .

Huikai et al have used bimorphs for biomedical applications<sup>15</sup>. They reported a single-crystalline silicon (SCS)-based micro-mirror with large scanning angle (up to 31 degrees) which can be used for biomedical imaging. The micro-mirror is fabricated by using a deep reactive-ion-etch (DRIE) and post-CMOS micromachining process. The micro-mirror is 1 mm by 1 mm in size, coated with aluminum, and thermally actuated by an integrated polysilicon heater. The radius of curvature of the mirror surface is about 50 cm. The micro-mirror showed the rotation of 31 degrees at 9 mA current. The resonant frequency of the device is 380 Hz.

Li-Hsin Han et al reported an experimental and theoretical investigation on a wireless BTA<sup>16</sup>. The developed BTA is actuated by a pulsed laser heating. The micro-machined BTA consisted of a thin gold layer deposited on a polysilicon base layer. A pulsed Nd:YAG laser of wavelength 355 nm and a pulse width of 12 ns was used to heat the BTA.

For microelectromechanical system (MEMS) applications, free of tight space constraints, BTA performance may in general be customized according to need through innovative or imaginative geometric layout and the use of compounded BTAs. Series compounded for enhanced deflection or parallel compounded for enhanced force. Tightly constrained applications such as DMD arrays and micro-fluidic control are performance-limited when using conventional approaches. Moreover, in elevated-temperature applications, these conventional materials may be

completely inapplicable.

**GOAL AND APPROACH**

This work presents on the enhancement in the actuation (force or displacement) of a bimorph cantilever actuator for a given geometry through the use of new materials and/or new fabrication process technologies. A survey

of candidate materials was performed, with particular attention paid to those characteristics relevant to the proposed new materials and new fabrication approaches, the operating behaviour of the device and the easy of accommodation into conventional fabrication processes.

Table 1 summarizes the important properties of several materials selected for the fabrication of a novel BTA.

**Table 1: Properties of materials of interest for Bimorph Thermal Actuators (BTA)<sup>17</sup>.**

Material	Coefficient of thermal expansion 10 <sup>-6</sup> /K	Young’s modulus 10 <sup>11</sup> N/m <sup>2</sup>	Specific heat kJ/kg k	Thermal conductivity W/m K	Density 10 <sup>3</sup> Kg/m <sup>3</sup>
Si	2.6	1.62	0.691	157	2.42
SiO <sub>2</sub>	0.4	0.74		1.4	2.66
Si <sub>3</sub> N <sub>4</sub>	2.8	1.55		19	3.2
SiC	3.5	4.57		350	3.2
Poly-Si	2.33	1.5	0.754	20-30	2.33
Al	25.0	0.7	0.9	236	2.7
Au	14.3	0.8	0.129	318	19.4
Pt	8.9	1.47	0.133	73	21.5
Cu	16.7	0.12	0.387	401	8.95
Ni	12.8	2.1	0.444	91	9.04
Pb	28.7	0.16	0.128	35	11.48
Stainless Steel	17.3	2.0	0.505	32.9	7.75

Among the candidate materials SiO<sub>2</sub> and Pb exhibit a large difference in thermal expansion coefficients and therefore are materials of interest as these could be used to achieve the objectives of large actuation, but need through analysis or simulation for justification.

The approach to accomplish the task is to select different combination of materials and then perform a comparison with respect to typically in these areas:

1. The radius of curvature of the beam (BTA), when it is subjected to temperature gradient.
2. The tip deflection of the BTA.
3. The equivalent force at the tip of the BTA.
4. Integration with electronics.
5. Mass producibility and manufacturing cost.
6. Application in the harsh environments.

**BROADER IMPACT**

The BTAs of Si-Steel, SiO<sub>2</sub>-Steel or Si<sub>3</sub>N<sub>4</sub>-Steel, could produce more actuation (large displacements and tip force). Moreover, these BTAs could be actuated over a long range of temperature and could also be operated at elevated temperatures, due to the high melting points of these materials. These characteristics permit some interesting application of these BTA in the harsh environment, where no other device could work or survive.

Some of the potential applications of these BTAs could be:

1. For the temperature sensing or monitoring in the harsh environment, such as, in nuclear reactors, steam generators, automobile engines, jet engines and chemical reactors.
2. For the switching in the harsh environment (as

a relay micro switch) for automation and control systems.

3. Multi degree actuation of DMD in projection devices and for the scanning in the harsh environment.
4. For large actuation of the AFM probe, moreover, the high tip force could be used to produce indentation in relatively hard materials.

## DESIGN, FABRICATION AND ANALYSIS

### Modeling

Figure 1 shows the schematic diagram of cantilever type BTA, with film layer on top of the base layer. Cantilever type BTA can be easily fabricated and are normally heated with an external source, such as, micro resistive heater. The undeflected BTA at room temperature, Figure 1(a), when heated with a micro resistive heat bends as shown in Figure 1(b). The radius of curvature of

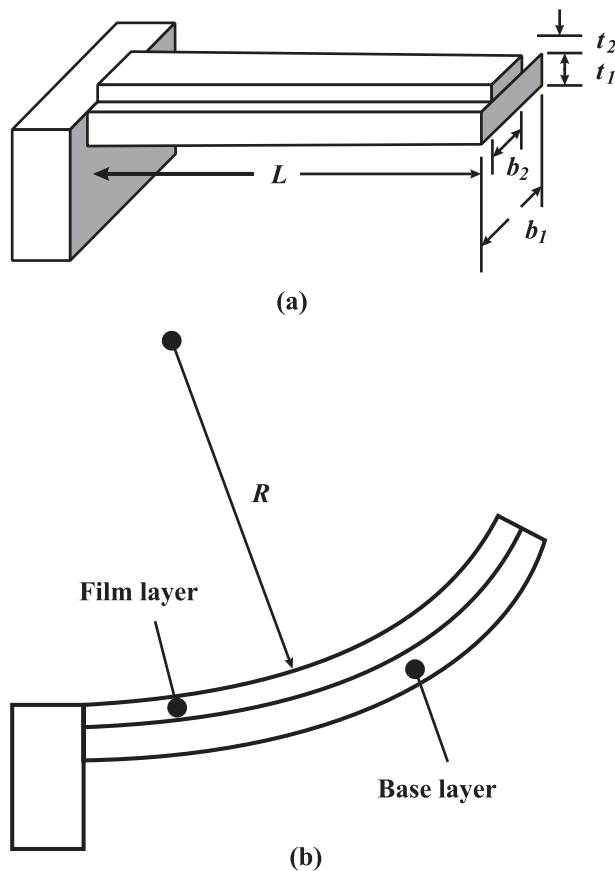


Figure 1: Schematic diagram of Bimorph thermal actuator: (a) Isometric view of BTA, (b) BTA during deflection.

the deflected BTA depends on the deflection of the beam. When the BTA is cooled back to the room temperature normally returns to its original position.

For cantilever type BTA with the radius of curvature  $R$  too large than the length  $L$  of the cantilever, that is ( $R \gg L$ ), the radius of curvature<sup>7</sup>

$$R = \frac{(b_1 E_1 t_1^2)^2 + (b_2 E_2 t_2^2) + 2b_1 b_2 E_1 E_2 t_1 t_2 (2t_1^2 + 3t_1 t_2 + 2t_2^2)}{6b_1 b_2 E_1 E_2 t_1 t_2 (t_1 + t_2) (\alpha_2 - \alpha_1) \Delta T} \quad (1)$$

can be obtained to a very good approximation.

Where

- $b_1$  = Width of base layer (beam)
- $b_2$  = Width of film layer
- $t_1$  = Thickness of base layer
- $t_2$  = Thickness of film layer
- $E_1$  = Young's modulus of base layer
- $E_2$  = Young's modulus of film layer
- $\alpha_1$  = Coefficient of expansion of base layer
- $\alpha_2$  = Coefficient of expansion of film layer
- $\Delta T$  = Temperature rise

The mismatch of thermal strains between the joined material layers produces a bending moment<sup>18</sup>

$$M = \frac{(EI)_{eff}}{R} \quad (2)$$

that depends on the effective flexural rigidity<sup>18</sup>

$$(EI)_{eff} = \frac{\hat{E}_1 b t_1^3}{12} + \frac{\hat{E}_2 b t_2 t_1^2}{4} \quad (3)$$

produced due to the effective (biaxial) young's modulus<sup>18</sup>

$$\hat{E} = \frac{E}{1 - \mu} \quad (4)$$

Of the beam, which is the function of the poisson ratio  $\mu$  and young's modulus  $E$  of the material.

The thermal stress<sup>18</sup>

$$\sigma = \frac{2M}{b_2 t_1 t_2} \tag{5}$$

produced in the thin film depends on the bending moment M,  $b_2$  = Width of film layer,  $t_1$  = Thickness of base layer  $t_2$  = Thickness of film layer

The tip deflection<sup>7</sup>

$$d = \frac{L^2}{2R} \tag{6}$$

of the BTA of length L, yields an expression for the equivalent tip force<sup>7</sup>

$$F_{eq} = \frac{3d(EI)_{eff}}{L^3} \tag{7}$$

generated at the tip of the bimorph cantilever beam.

**Design constraints**

For large actuations, materials with large difference in the co-efficient of thermal expansion must be selected. In such a choice, the cantilever actuation then depends only on the materials young’s modulus and the temperature rise. Theoretically actuation is proportional to the temperature rise. As the temperature is raised the beam actuation will increase. However, in fact, due to the physical and mechanical properties of the selected layers there are some limitations imposed on the actuation. These design constraints for the BTA are:

1. Melting point of the materials,
2. Yield strength of the materials and
3. Mathematical Model constraint ( $R \gg L$ )

The above mentioned constraints for different bimorph materials are tabulated in Table 2.

**Simulation of Bimorph thermal actuator**

For BTA, to obtain the materials of choice that produces enhanced actuation, different combinations of materials are simulated for the tip deflection and actuation

**Table 2: Melting point and yield strength of different film materials.**

Film Material	Melting point (k)	Yield strength (MPa)
Au	1337.33	200
Pb	600.6	12
Al	933.5	170
Cu	1357.8	62
Ni	1728	140
Stainless Steel	1700	2100
Si3N4	2173	14000
SiO2	1873	8400
Si	1687	7000

force as a function of temperature rise. Equations (1) to (7) are utilized to perform the simulations. For a simulation purposes, the dimensions of a typical BTA are given in Table 3.

**Table 3: Dimensions of the simulated BTA.**

Parameter	Value (µm)
Thickness of base layer ( $t1$ )	1.5
Thickness of film layer ( $t2$ )	0.5
Width of base layer ( $b1$ )	80
Width of film layer ( $b2$ )	70
Length of bimorph ( $L$ )	300

Figure 2 shows the tip deflection of different combination of materials for BTA as a function of temperature rise. Equations (1) and (6) are used to compute the tip deflections and obtain the plot. The simulation result shows as the temperature is increased the tip deflection increases indefinitely and it seems that the SiO<sub>2</sub> and Al is the best combination for BTA. However, in fact the BTA deflection is restricted by the above mentioned constraints. The yield strength of the film actually limits the maximum actuation of the BTA. When the temperature is raised, not only the tip deflection increases but also the bending stress in the film increases. When the stress in the film layer increases beyond the yield strength of the film, permanent set will occur in the film and upon cooling the BTA will not return back to its initial (starting) position. The yield strength of the film or base layer, whichever is the less, is a design constraint that limits the BTA actuation and must be incorporated in the material selection for the proposed BTA.

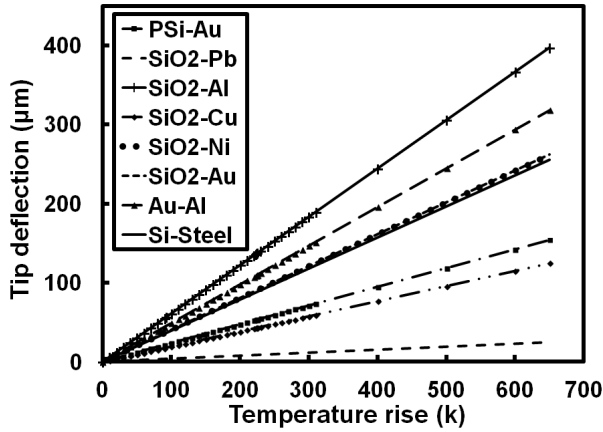


Figure 2: Tip deflection as function of temperature rise without design constraints.

The temperature at which the stress in the film layer becomes equal to the yield strength of the film material is the critical temperature. At the critical temperature permanent deformation (yielding) will take place in the film layer. Thus forth, for proper operation of the BTA, it not needs to be operated up to and beyond the critical temperature of the film layer. Figure 3 shows the simulation of the tip deflection of different BTAs while incorporating the critical temperature of film layer. The yield strength constraint limits the operation range of BTAs. The polysilicon-gold (Psi-Au) BTA, which previously seemed the best combination of base and film layer, is actually not the best choice for the enhanced actuation for the BTA. The simulation results, in Figure 3, indicate that Si-Steel BTA can be actuated to larger tip deflection due to the higher yield strength of steel (2100 MPa). A maximum tip deflection of about 255 µm can be obtained with a bimorph that have steel as film layer.

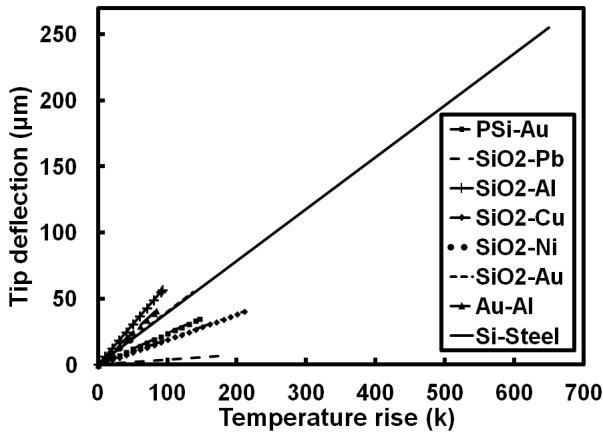


Figure 3: Tip deflection after yield strength constraint.

When the constraint,  $R > L$ , is utilized during the simulation, the result is shown in Figure 4. Based on this constraint a maximum of 86.4 µm tip deflection would be produced by the Si-SS BTA.

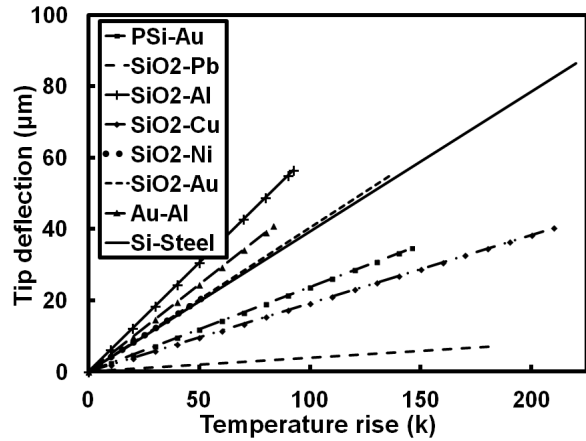


Figure 4: Tip deflection after  $R > L$  constraint.

Figure 4 and Figure 5 show the force produce by the tip of the BTA based on the yield and  $R > L$  constraints respectively.

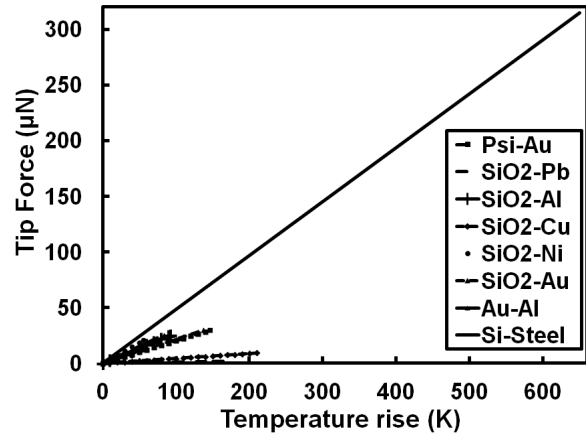


Figure 5: Tip force after yield strength constraint.

With the yield strength constraint a maximum of 315 µN is obtained. However,  $R > L$ , constraint restricted the tip force to a maximum of 107 µN. The above graphs show that under same conditions the bimorph of choice should be Si-Stainless Steel, specifically under conditions where  $SiO_2$ -Al fails. The Si-Stainless Steel bimorph will give more deflection and force than the other bimorphs and the reason for this is the high yield strengths of the stainless steel (2.1 GPa) and silicon (7 GPa). So theoretically it is possible to deflect this bimorph close to the yield strength of the S.S but it is more likely

that the bonding or adhesion between bimorph layers will fail before that point is reached. The accuracy of the deflection of SS-Si is also limited by the modeling constraint that is  $R \gg L$ .

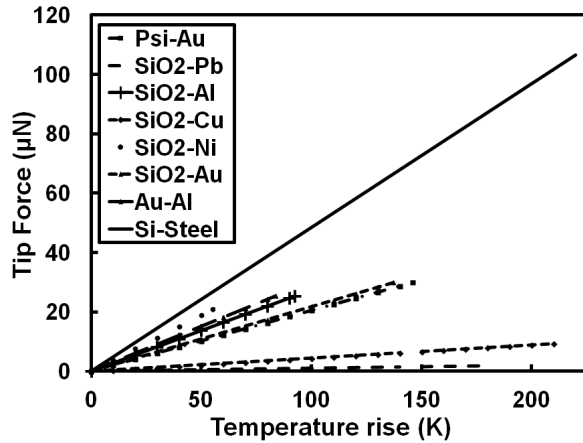


Figure 6: Tip force after  $R > L$  constraint.

The simulation results for different bimorphs are summarized in table 4.

Table 4 shows the summarized simulation result after the application of the constraints and its quite evident that  $\text{SiO}_2$ -Al bimorph is not the universal best choice but that Si-Stainless Steel bimorphs provide opportunity for actuation enhancement.

### Proposed Fabrication

Since stainless steel is involved as the structural layer in the device. For the deposition and etching of SS it is not possible to utilize the standard IC and Si-based fabrication techniques and technologies. However, a number of process technologies that are available for industrial production can be explored to produce the Si-SS BTA. Moreover, it is also important that the selected process

Table 4: Summary of simulation results.

Beam	Film	$T_{max}$ (K)	R ( $\mu\text{m}$ )	d ( $\mu\text{m}$ )	$F_{eq}$ ( $\mu\text{N}$ )
Poly Silicon	Au	446	1299.2	34.6	29.9
SiO2	Pb	481	6432.5	7	1.79
SiO2	Al	392.5	796.6	56.5	25.4
SiO2	Cu	510	1117.1	40.3	9.29
SiO2	Ni	355	2037.6	22.1	20.9
SiO2	Au	437	815.6	55.2	29.9
Au	Al	383.5	1101.2	40.9	25.4
Si*	Steel*	520*	520.7*	86.4*	107*
Si^	Steel^	950^	176.3^	255^	315^

\* Values are based on the modeling constraint ( $R \gg L$ ).

^ Values based on the yield strength constraint of the Steel.

technology or the developed fabrication technique must be versatile enough to accomplish for the product with the requirements of reproducibility, batch production and cost effectiveness. In one way to fabricate the Si-SS BTA, following could be the fabrication steps:

1. Etching of Si wafer
2. Deposition of Stainless steel on Si wafer
3. Generation of Cantilever bimorph in the composite wafer
4. Integration with the micro electronics

### Etching of Si wafer

The Si wafer is used as the base layer, and therefore the thickness of the Si wafer will be reduced to  $1.5 \mu\text{m}$  by etching the wafer. A number of fabrication techniques are available and could be used to perform the etching of Si wafer. Anisotropic etching of Si wafer could be performed with etchants like KOH, EDP or TMAH. During the fabrication the etching can be stopped by either with Boron doping (by ion implantation) as etch stop region or with Electrochemical etch stopping. However, alternatively deep reactive ion etching (DRIE) can be

utilized as a fabrication process to produce a 1.5 μm thick Si base layer in wafer. The outcome of the etching of Si wafer is shown in Figure 6.

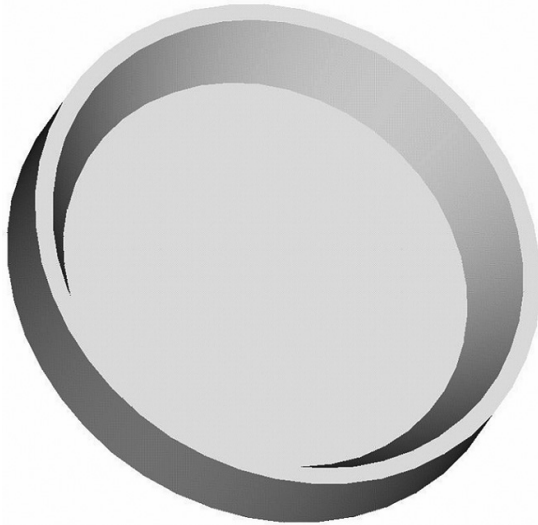


Figure 7: Etched Si wafer.

**Deposition of Stainless steel on Si wafer**

The deposition of thin film of SS on Si wafer could be performed either with (a) RF magnetron sputtering or (b) Pulse laser deposition.

**(a) RF Magnetron Sputtering**

Thin SS films could be deposited on Si wafer by a RF magnetron sputtering method. In this method using SS material as the target and Argon (Ar) gas as sputtering gas, a high quality SS layers can be obtained on Si substrate. The quality of the deposited thin film largely depends on substrate temperature and the distance between target and substrate. Moreover, the concentration of N<sub>2</sub> gas in Ar, controls the phase and crystalline structure (BCC ferrite or FCC austenite) of deposited SS layer. Afterward SS deposition, annealing can be performed to reduce the residual stresses in the deposited film<sup>19, 20</sup>. Process Parameters for this deposition are listed in Table 5.

**(b) Pulse Laser Deposition (PLD)**

Pulse laser deposition could also be used to deposit the SS film on the Si substrate. In this process the target material (SS) is ablated by a laser and the plume of the ablated material is allowed to deposit on the substrate

**Table 5: Process parameters during RF Magnetron Sputtering for Stainless steel deposition.**

Description	Parameters
Target	Stainless Steel
Sputter gas	Ar or Ar-N <sub>2</sub> mixture
RF power	200 W
Distance between target and substrate	40 – 150 mm
Ar pressure	0.5 – 0.6 Pa
Substrate temperature	100 – 400oC
Annealing	400 – 600oC, 1hour

(Si) located directly opposite to the target. During the process the laser is inclined at 45° to the target and also the target is rotated at specific rpm<sup>21</sup>. In this process parameters that need to be controlled are excimer Laser (KrF ,248nm), laser pulse duration (ns/ fs), frequency (Hz), energy per pulse, fluence, substrate temperature, target-Substrate distance, base Vacuum and post deposition annealing. The deposited layer of SS on Si is shown in Figure 7.

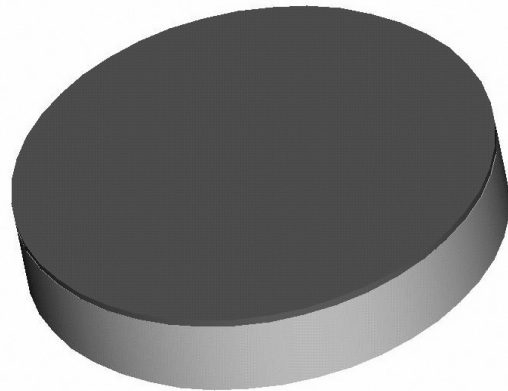


Figure 8: SS deposited on the etched Si wafer.

**Generation of Cantilever bimorph in the composite wafer**

In the composite wafer of SS and Si, the cantilever bimorph beam could be now produced by laser ablation (LA) or by Micro Electric Discharge Machining (μEDM).

**(a) Laser Ablation**

High power diode pumped solid-state laser (Nd:YAG or Nd:YVO<sub>4</sub>) with nano and femto second pulses and with specific fluence could be used to ablate the SS and Si layers. The process parameters depend on the material

and the thickness of each layer to be removed. For SS and Si the process parameters will be different from each other and therefore should be adjusted according to specific material. As the ultrafast lasers, such as, pico seconds and femto seconds laser beam offer superior quality during micromachining, are preferred during micromachining<sup>22, 23, 24</sup>. The process parameters for the ablation of SS and Si layers are listed in Table 6. The wafer after laser ablation is shown in Figure 8.

**(b) Micro Electric Discharge Machining**

Micro electric discharge machining ( $\mu$ EDM) could also be used to produce the bimorph cantilevers in the composite wafer. Both EDM milling and die-sinking

**Table 6: Process parameters during ablation of SS and Si layers.**

Parameter	Material layer	
	Stainless Steel	Si
Laser	Nd:YAG	Nd:YAG
Wavelength	532nm	355nm
Pulse energy	2.5 mJ	
Pulse width	15 ns	12 ns
Fluence	890 J/cm <sup>2</sup>	
Frequency		50 KHz
Power		5 W

EDM could be used to accomplish the task. However, the latter has the advantage, to be easily transformed in to the batch fabrication.

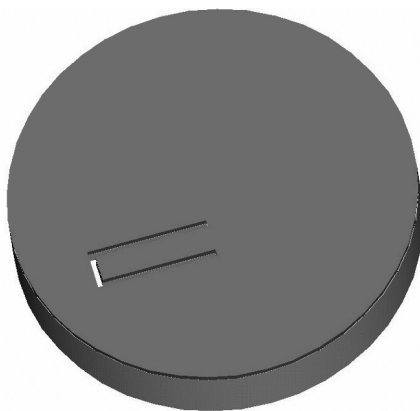


Figure 9: Cantilever BTA produced by Laser Ablation or  $\mu$ EDM.

**(i) By EDM milling**

Cylindrical electrode of Tungsten could be used to make the slits by the precise movement of the work piece. Being a serial process, it will be cost effective only to make prototypes.

**(ii) By Die-Sinking EDM (Batch Micro EDM)**

In this method first a LIGA-fabricated array of copper (Cu) electrodes is to be produced on the Si substrate<sup>25</sup>, using the monolithic electrode approach as shown in the Figure 9.

This method provides high throughput, which leads to batch fabrication.

To generate the bimorph cantilever beams, the overall thickness to be machined is small (only 2  $\mu$ m), so for producing 4  $\mu$ m to 10  $\mu$ m high Cu electrodes, the low cost technique, SU8, should be utilized. This would considerably decrease the production cost of Cu electrodes array and also the overall cost of the final product (due to the elimination of the use of expensive LIGA process).

The process parameters that control the material removal rate (MRR) and the surface finish are voltage, discharge capacitance and feed rate. Obviously for high efficiency these parameters should be adjusted differently for SS and Si layers. Moreover, a new technique for decreasing machining time or increasing MRR was developed by<sup>26</sup>, in which ultrasonic vibration to the work piece is provided. The ultrasonic vibrations improve the dielectric oil circulation and debris removal, which results in better surface finish and quick machining.

**Batch Fabrication**

In order to increase the throughput, batch fabrication of the devices should be performed, as shown in Figure 10. Batch processing of such BTAs are possible with  $\mu$ EDM. In  $\mu$ EDM batch processing could be obtained by parallel discharge machining during which multi timing circuits are used. Also with the use of monolithically fabricated Cu electrodes array and by exploiting the parasitic capacitance, very smooth and high quality surfaces could be achieved.

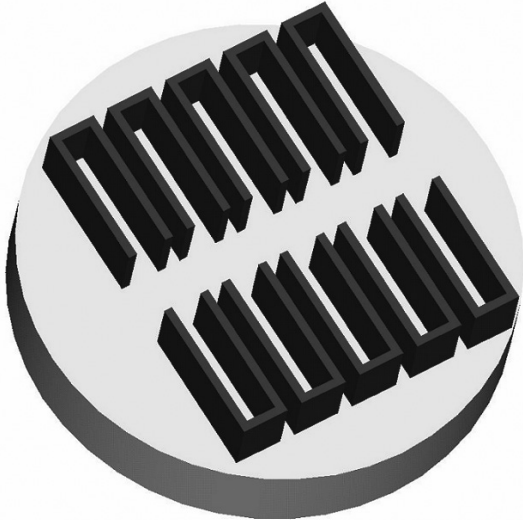


Figure 10: Copper electrodes array on Si substrate.

For harsh environment applications, silicon carbide (SiC) needs to be used for the fabrication of electronic circuitry. Being having a very high melting point and the other properties close to Si, SiC as a material for interconnects is the promising choice.

**Bimorph Thermal Actuated Micromirror**

Si-SS BTA DMD could be fabricated by the same generic processing steps. The advantage of Si-SS BTA DMD would be large actuation (angular displacements) and operation in high temperature environments due to the high melting points of both Si and SS. The solid models of such DMDs are shown in Figure 11, Figure 12 and Figure 13.

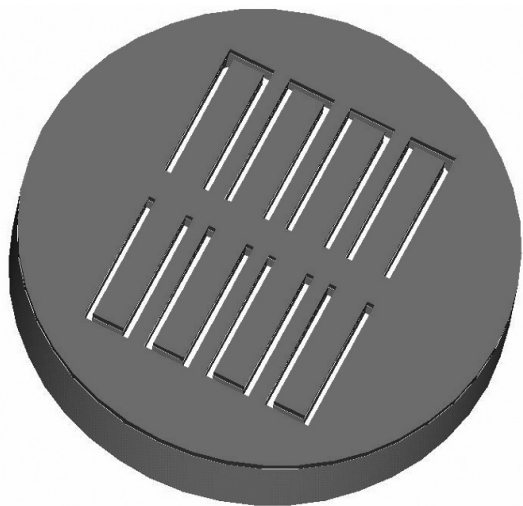


Figure 11: Batch fabricated BTAs.

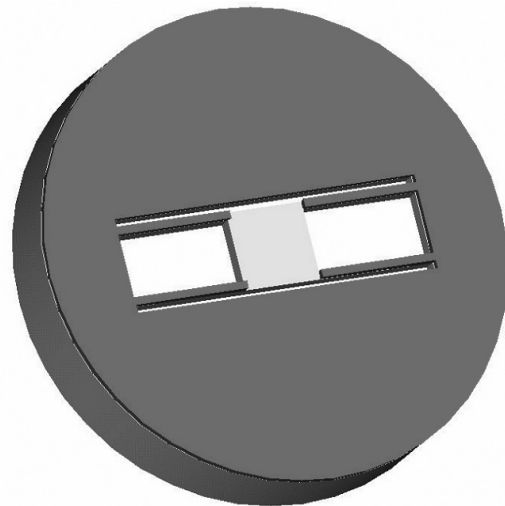


Figure 12: DMD with parallel BTAs.

By laser micromaching the processing time could be decreased with mask projection techniques, such as, work piece or Mask Dragging Technique and synchronized Scanning Technique.

**Integration with the micro-electronics**

Micro-electronics could be fabricated on both sides of the substrate that is on Si (bottom) side or on top SS side. The selective etching of only SS layer could be done with Laser ablation. Moreover, with photoresist or Si<sub>3</sub>N<sub>4</sub> as mask, the SS layer etching could also be performed by wet immersion etching or spray etching of ferric chloride (FeCl<sub>3</sub>).

For the DMD shown in Figure 11, when all the BTAs are actuated it will move out of plane (piston like motion). However, when the two adjacent BTAs are actuated then it will rotate about the wafer plane (angular displacement of the mirror will be obtained).

In the design of DMD shown in Figure 12, when only one BTA is actuated, angular displacement can be obtained. The two unactuated BTAs perpendicular to the actuated BTA will work as torsion bars (springs). This DMD could be actuated in two directions that is about x-axis and y-axis. Moreover, because of the cross orientation of the BTAs, the structure is more stable than that shown in Figure 11.

In order to further increase the angular displacement of the DMD another unique design is shown in Figure 13. In this design the film is deposited on the opposite sides of cross BTAs. When the cross BTAs are actuated, these will move in opposite direction and deflect the micro mirror through more angular displacement. This DMD could also be actuated in two directions that is, about x-axis and y-axis.

**DEVICE PERFORMANCE**

Austenitic steels, which includes a wide range of alloy considered as stainless steel and exhibit a significantly

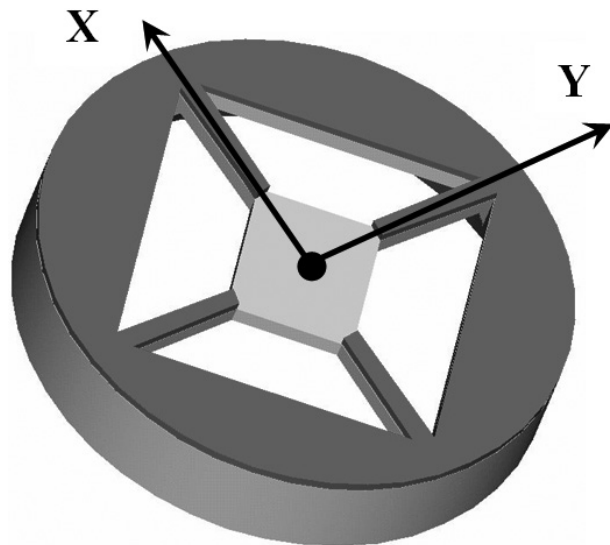


Figure 13: DMD with cross BTAs.

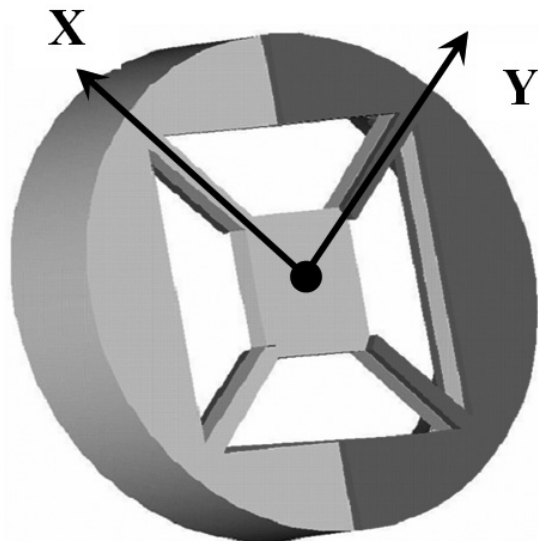


Figure 14: DMD with cross-opposite film-deposited BTAs.

higher coefficient of thermal expansion ( $\sim 17 \times 10^{-6} \text{ 1/K}$ ) as compared to other steel types ( $\sim 12 \times 10^{-6} \text{ 1/K}$ ). In addition to their high material strength, melting temperature and yield strength, austenitic steels are attractive material candidates for extreme and harsh condition MEMS BTAs. The utility of these actuators is not limited solely to extreme environments. It is not so difficult to imagine a circumstance where the high available forces of such a BTA may prove useful. Indeed, whenever a design constraint faced by MEMS designers may be mitigated there exist an opportunity for innovative design and an expanded field of potential applications. We can broadly categorize  $\text{SiO}_2\text{-SS}$  BTA applications into a high temperature environment applications and extreme actuation applications.

High temperature environments quickly restrict material choices for BTAs. For instance, even a  $\text{SiO}_2\text{-Al}$ , BTA should not be intended for use in a high temperature environment, it is impractical to attempt to restrict the temperature swings that such a device would exposed to during fabrication and field installation. Plastic deformation would be unavoidable and deflections so large (compared to usable temperature swings during operation) that layout geometry could be problematic. Only with material choices such as  $\text{SiO}_2\text{-SS}$  could have a device that reside at ambient temperature (say  $25^\circ\text{C}$ ) and then can be exposed to temperatures of several hundred degrees and remain operative without severe difficulties.

Figure 14 shows the performance of the  $\text{SiO}_2\text{-Al}$  and  $\text{Si-SS}$  BTAs when they are actuated up to the same tip deflection. The comparison is done up to the critical temperature of the Al layer. Due to high thermal conductivity of the Al, the  $\text{SiO}_2\text{-Al}$  actuation is more efficient and relatively at lower temperature rise. As shown in Figure 14, for the same tip deflection a  $\text{SiO}_2\text{-SS}$  BTA requires approximately 55 % larger temperature increase. For actuation application less than  $57 \mu\text{m}$  tip deflection, the  $\text{SiO}_2\text{-Al}$  BTA is the better choice. Under this circumstance the use of  $\text{Si-SS}$  BTA would lead to more energy consumption and a larger micro resistive heater for heating.

The heat capacity C, thermal conductivity K, density  $\rho$  of SS and Al are shown in table 7.

For identical volumes (dimensions), the ratio of stored thermal energies for equivalent deflection is obtained by

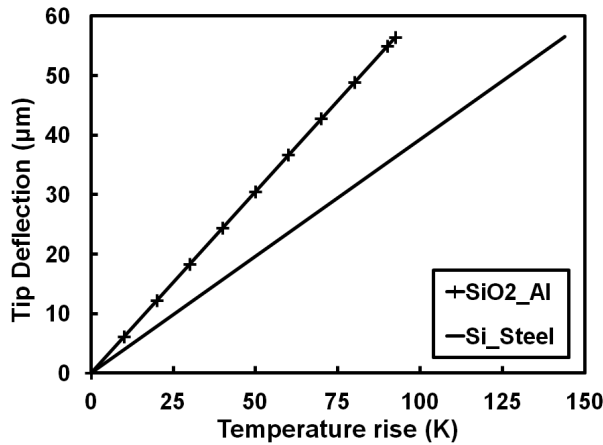


Figure 15: Comparison of Al and SS films on SiO<sub>2</sub>.

Table 7: Thermal Properties of SS and Al.

Material	C (J/kgK)	K (W/mK)	ρ (kg/m <sup>3</sup> )
SS	475	44.5	7850
Al	904	237	2700

$$\frac{Q_{ss}}{Q_{Al}} = \frac{(\rho C \Delta T)_{SS}}{(\rho C \Delta T)_{Al}} = \frac{7850 \times 475 \times 144}{2700 \times 904 \times 93} = 2.37$$

Indicating that for equivalent tip deflection twice as much energy is required by SS in comparison to Al. However, at equivalent deflection, the tip force available from SS film as compared to Al film is simply the ratio of Youngs' moduli. This means that the SS film provides 2.0 / 0.69 = 2.9 times as much force as that of Al film.

A similar analysis of the response time constants τ of SS and Al may be performed, where the ratios are related by

$$\frac{\tau_{SS}}{\tau_{Al}} = \frac{\rho_{SS} K_{Al}}{\rho_{Al} K_{SS}} = 15.5$$

The time response of BTA with SS as film material is almost 15.5 times faster than that with Al as a film layer. The quick response of the BTA is significant for fast switching and scanning.

Interfacing to electronics is no different for SS BTAs from Al BTAs, should they be resistively heated at the base as is typical.

### DISCUSSION

For small actuations SiO<sub>2</sub>-Al is the preferable choice. However, for large actuations and high temperature environments, the SS film on Si, poly Si, SiO<sub>2</sub>, Si<sub>3</sub>N<sub>4</sub> or SiC forms the promising BTA. Although it is not easy to deposit SS, as it is an alloy and composition and characteristics of the deposited layer is not necessary to be the same, which will then affect the performance of the BTA. One way to overcome this problem is to use SS substrate (25 µm thickness. SS wafer), its thickness could be decreased by chemical mechanical polishing (CMP) and the other layer could be then deposited by standard IC fabrication techniques.

Due to the application of the process techniques, like micro EDM, PLD and Laser Ablation, decrease the throughput and increase the cost of the device. Although the batch fabrication of the devices mentioned in the fabrication step would increase the throughput, but still some more research is required to optimize the fabrication process.

As the coefficient of volume expansion β is three times more than the coefficient of linear expansion α,

(β = 3α), this phenomenon could be utilized to further improve the performance of the device (in other words to move from the 2D to 3D structure). With 3D fabrication of the BTA as shown in Figure 16, extremely significant actuations can be expected.

Moreover, polymers such as polyamide, polyoxymethylene and PMMA could also be used as film layers,

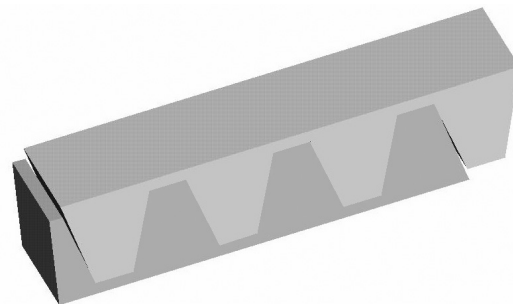


Figure 16: 3D Bimorph Thermal Actuator (β=3α).

in order to increase the actuation but the problem is their poor thermal conductivities and specific heats as compare to metals, this would make the response time of the actuator too long, which would be not desirable in a number of applications.

## CONCLUSION

The actuation enhancement of a bimorph thermal actuator (BTA) is investigated in this research work. For BTA, the reported analytical models have been used to obtain the materials of choice that could produce maximum actuation as well as have the tendency to be used in harsh environments, such as, in nuclear reactors, steam generators, automobile engines, jet engines and chemical reactors. The simulation results showed that for BTA, among several material combinations, the BTA composed of Si-Steel produced large tip deflection and high equivalent force. For Si-Stainless steel (Si-SS) BTA, based on the yield strength constraint of the film (SS) layer, the tip deflection of 255  $\mu\text{m}$  and an equivalent force of 315  $\mu\text{N}$  are obtained when the BTA is heated up to the temperature rise of 950 k. However, when the constraint  $R > L$ , is incorporated the simulation results predicted a tip deflection of 86.4  $\mu\text{m}$  and an equivalent force of 107  $\mu\text{N}$  for a temperature rise of 520 k.

For the fabrication of a novel Si-Steel BTA, a generic fabrication process is described based on the product (BTA), reproducibility, batch fabrication, applicability, mass production and cost effectiveness. In the described generic fabrication process, the micro-fabrication technologies, such as Pulsed Laser Deposition (PLD), Laser Ablation (LA) and micro electro-discharge machining ( $\mu\text{EDM}$ ) are utilized to produce Si-Steel BTA. The fabrication of different designs of bimorph thermally actuated digital micro-mirror devices (DMDs) are also described by the same generic fabrication process in order to show the practical utility of this research in the field of MEMS. The DMDs actuated by BTAs, are easy to fabricate and can scan through larger angles as compared to the normally used electrostatically actuated DMDs.

The BTAs of Si-Steel,  $\text{SiO}_2$ -Steel or  $\text{Si}_3\text{N}_4$ -Steel, produce more actuation and could survive in high temperature environment. Some probable applications may include, temperature sensing or monitoring in harsh environments, such as, in nuclear reactors, boilers,

automobile engines, jet engines, aircrafts and chemical reactors. Moreover, these could be used as a relay micro-switch, for switching in a harsh environment. For multi-degree actuation of DMD in media devices or for scanning in a harsh environment these BTAs could have also the utilization. For actuation of AFM probe tips, the high tip force could be used to produce indentation in relatively hard materials.

## REFERENCES

1. Nicholas, J. C., Zachary, J. T. and Sang, G. K., 2007. "A strain amplifying piezoelectric MEMS actuator". *J. Micromech. Microeng.* 17 (4): 781. doi:10.1088/0960-1317/17/4/015.
2. Subrahmanyam, G., Atanu M. and Anindya C., 2006. "Cantilever beam electrostatic MEMS actuators beyond pull-in". *J. Micromech. Microeng.* 16 (7): 1800 doi:10.1088/0960-1317/16/9/007.
3. Reid, J., Bright, V., and Comtois, J., 1997. "Force measurements of a polysilicon thermal micro-actuator", *Proc. SPIE* 2882: 296–306.
4. Getprecharsawas, J., Puchades, I., Hournbuckle, B., Fuller, L., Pearson, R., and Lyshevski S., 2006. "An electromagnetic MEMS actuator for micropumps". *Proc. MEMSTECH*, 1: 11–14.
5. Doring, C., Grauer, T., Marek, J., Mettner, M. S., Trah, H. P. And Willmann, M., 1992. "Micromachined thermoelectrically driven cantilever structures for fluid jet deflection". *Proc. IEEE MEMS Workshop (MEMS'92)*, pp.12 -18.
6. Riethmuller, W. and Benecke, W., 1988. "Thermally excited silicon microactuators". *IEEE Transactions on Electron Devices* 35(6):758–63.
7. Chu, W. H., Mehregany M., and Mullen, R.L., 1993. "Analysis of tip deflection and force of a bimetallic cantilever microactuator". *Journal of Micromechanics and Microengineering*, 3(1): 4–7.
8. Dong, Y., Khajepour, A. and Mansour, R., 2003. "Modeling of two-hot-arm horizontal thermal actuator". *Journal of Micromechanics and*

*Microengineering*, 13(2): 312–22.

Academic Publishers, Boston, USA.

9. Dong, Y., Khajepour, A. and Mansour, R., 2004. "Design and modeling of a MEMS bidirectional vertical thermal actuator". *Journal of Micromechanics and Microengineering* 14(7): 841–50.
10. Yan, D., Khajepour, A. and Mansour, R., 2002. "Mechanical design and modeling of a new MEMS vertical actuator". *27th Biennial Mechanisms and Robotics Conference, Montreal, Quebec, Canada* 5: 813-817.
11. Liu, G. And Oh, S., "A Stress-Induced Thermal actuator for Optical Purpose". [Online]. Available from <http://robotics.eecs.berkeley.edu/~pister/245/project/LiuOh.pdf> [cited 4 August 2014].
12. Bullen, D., Zhang, M. and Liu, C., 2002. "Thermal-mechanical optimization of thermally actuated cantilever arrays". *SPIE 9th Annual Int. Symp. Smart Structures and Materials*, pp. 17–21.
13. Jain, A., Qu, H., Todd, S. and Xie, H., 2005. "A thermal bimorph micromirror with large bi-directional and vertical actuation". *Sensors and Actuators A* 122:9–15.
14. Todd, S. T., Jain, A., Qu, H. and Xie, H., 2005. "A 3-D Micromirror Utilizing Inverted-Series-Connected Electrothermal Bimorph Actuators for Piston and Tilt Motion". *Proc. Optical MEMS and Their Applications* pp. 27–28.
15. Xie, H., Jain, A., Xie, T., Pan, Y. and Fedder, G. K., 2003. "A single-crystal silicon-based micromirror with large scanning angle for biomedical applications". *Proc. Tech. Dig. CLEO*, pp. 858–860.
16. Han, L. H. and Chen, S., 2005. "Wireless bimorph micro-actuators by pulsed laser heating". *Sensors and Actuators A* 121:35–43.
17. Gregory, T.A.K. 1998. "Micromachined transducers sourcebook". *International editions 2000, McGraw-Hill, New York, USA*.
18. Senturia, S.D., 2001. "Microsystem design". *Kluwer Academic Publishers, Boston, USA*.
19. Nomura, K., Iio, S., Ujihira, Y. and Terai, T., 2005. "DCEMS Study of Thin Stainless Steel Films Deposited by RF Sputtering of AISI316L" *AIP Conf. Proc.* 765, 108.
20. Zhang, X. and Misra, A., 2004. "Residual stresses in sputter-deposited copper/330 stainless steel multilayers". *J. Appl. Phys.* 96:7173–7178.
21. Nomura, K., Yamada, Y., Tomita, R., Yajima, T., Shimizu, K. and Mashlan, M., 2005. "CEMS Study of Stainless Steel Films Deposited by Pulsed Laser Ablation of AISI316". *Czechoslovak Journal of Physics* 55(7): 845–852.
22. Bensaoula, A., Boney, C., Pillai, R., Shafeev, G.A., Simakin, A.V., Starikov, D., 2004. "Arrays of 3D micro-columns generated by laser ablation of Ta and steel: modelling of a black body emitter" *Appl. Phys. A* 79: 973-975.
23. Henry, M., Harrison, P. M., Henderson, I. and Brownell, M. F., 2004. "Laser milling – A practical industrial solution for machining a wide variety of materials". *Fifth International Symposium on Laser Precision Microfabrication*, 627: doi:10.1117/12.596743.
24. Banks, P.S., Stuart, B.C., Komashko, A.M., Feit, M.D., Rubenchik, A.M., & Perry, M.D., 2000. "Femtosecond Laser Materials Processing," *Proc. SPIE* 3934, p.14.
25. Takahata, K., Shibaiki, N. and Guckel, H., 1999. "A novel micro electro-discharge machining method using electrodes fabricated by the LIGA process". *Tech. Dig. IEEE Int. Conf. on Micro Electro Mechanical Systems (MEMS'99)*, pp.238–243.
26. Kim, D. J., Yi, S. M., Lee, Y. S. and Chu, C. N., 2006. "Straight hole micro EDM with a cylindrical tool using a variable capacitance method accompanied by ultrasonic vibration". *J. Micromech. Microeng.* 16:1092–1097.